Kelly, C.J., Wysk, R.A., Harrysson, O.A., King, R.E., & McConnell, B.M. 2024. Automatic Feature Based Inspection and Qualification for Additively Manufactured Parts with Critical Tolerances, *International Journal of Manufacturing Technology and Management*, Vol 38, No 3, 236–264.
http://dx.doi.org/10.1504/IJMTM.2023.10059964

Automatic Feature Based Inspection and Qualification for Additively Manufactured Parts with Critical Tolerances

Christopher J. Kelly[1], Richard A. Wysk[2], Ola A. Harrysson[2], Russell E. King[2], and Brandon M. McConnell[2,*]

[1]Celonis, Raleigh, North Carolina, USA
[2]Center for Additive Manufacturing and Logistics (CAMAL), North Carolina State University, Raleigh, North Carolina, USA
[*]Corresponding author: mcconnell@ncsu.edu

Abstract

This work expands the capabilities of the Digital Additive and Subtractive Hybrid (DASH) system by including "geometric qualification" of mechanical products. Specifically, this research incorporates the extended Additive Manufacturing Format files (AMF-TOL) which include American Society of Mechanical Engineers (ASME) Y14.5 specifications for planes, cylinders and other features so that "in-process" inspection can be completed automatically. An example for the production of holes is provided to illustrate On-Machine-Measurement collects sample radii to estimate the size and position of finished cylindrical features. Statistical analysis was used to measure bounds for comparison to specified tolerance callouts to determine whether a part is within specification, within a user-defined level of confidence. Seven different sampling strategies were evaluated on a DASH part including the bird cage sampling strategy defined in ISO-12180. Part data was utilized to show that for large data samples no statistically significant difference in accuracy was identified for four methods. Finally, analysis shows that using the DASH process with automatic inspection is economically advantageous for low volume production runs.

Keywords: Additive manufacturing, CNC machining, Hybrid manufacturing, Inspection

1 Introduction

There are a number of applications for the production of parts in small lots including low volume products and spare part production (Bromberger et al., 2022). Often these parts have geometric complexity and critical tolerances. In this environment, additive manufacturing (AM) has been shown to provide advantages over traditional manufacturing in terms of costs (Khajavi et al., 2018; Li et al., 2019; Keefer, 2020; 3DEO, 2022). However, the ability to automatically finish AM-produced parts to tolerance specification without specialized tooling has been a challenge.

An approach termed the Digital Additive and Subtractive Hybrid (DASH) system, developed as a collaboration between researchers at North Carolina State University and Iowa State University, is a method to combine the geometrical benefits and ability to quickly create custom parts through AM with the accuracy of traditionally machined surfaces. This method provides a platform for the user to specify critical features and tolerances of a part, add machining allowance, print the part, then machine the critically marked surfaces using a traditional milling machine equipped with a 4th rotational axis (Srinivasan, 2014).

At this point, the part would typically be removed from the machine, and manually measured for accuracy of critically toleranced surfaces. An important subset of features includes circles and cylinders. The focus of this work is to eliminate this manual setup for metrology of these features and replace it with a set of procedures to automatically measure the part while still on the Computer Numerical Control (CNC) machine.

Several methods have been developed to improve the accuracy of additive manufactured parts. One of the methods that has been developed employs a concept called CNC-RM (Frank et al., 2005, 2006). This

concept utilizes a layer by layer CNC machining process (like that used in AM) but to remove material rather than to deposit it. CNC-RM is a manufacturing process that is capable of producing metal parts with high precision and reliable quality, whereas many additive manufacturing methods are less capable in these respects. It uses a layer-removal methodology to machine parts from a "bar stock" billet just larger than the required part, and utilizes an indexing device to clamp the workpiece, which can be used to extend CNC applications into the realm of rapid manufacturing (CNC-RM) processes. CNC-RM enhances process accuracy by minimizing the staircasing effect of layer removal so as to improve the quality of machined parts. In order to achieve this, different types of end mill tools are introduced to cater for specific part surfaces during finishing operations. CNC-RM has moved from a research method to industry and the concept is currently being used by several industries including John Deere (Deere, 2022). This methodology was also expanded to components that would be manufactured using Electric Discharge Machining (EDM) in place of traditional machining (Yang et al., 2011, 2009, 2012).

A drawback for CNC-RM is that depending on the part geometry, the process can be wasteful in terms of raw material usage. It also has the disadvantage that the part geometry is limited to geometries that can be produced via machining. In order to eliminate these deficiencies, Manogharan (2014) demonstrated that CNC-RM could also be used to machine AM produced parts by adding sacrificial machine fixtures to the raw AM component (Manogharan et al., 2016, 2015). This eliminated much of the material waste as well as geometric limitations. Srinivasan (2014) further expanded the system so that AM components could be "automatically located on the CNC machine and finished" using CNC-RM to the exacting AM built component geometry (Srinivasan et al., 2015a,b). The logical next step to extend this application to one-of-a-kind and very low volume mechanical parts is to also include in-situ product inspection to the process.

The major contribution of this paper is to show how this can be accomplished and how it fits within the context of Smart Manufacturing methods. Our early investigation of in-situ probing of planar components is reasonably straightforward as "limiting feature conditions" can simply be collected and all of the sampled points need to reside within these conditions. That is, planes and their tolerance specifics are well defined using International Organization for Standardization (ISO) 12180 standard definitions for flatness (International Organization for Standardization (ISO), 2023; Janecki et al., 2015). The definition is specified using limiting conditions, which makes their inspection easy. All planar surfaces produced using CNC-RM can be inspected and certified using a touch probe or a laser scanner directly. Furthermore as a requirement for using CNC-RM, these surfaces need to be "visible" to be accessible by a rotating tool. It follows that they can be accessed using a normal from the surface and a standard probe.

Nonplanar surfaces however introduce a number of other difficulties. In this paper, we have selected cylindrical surfaces as the next geometric feature to investigate. This direction can be justified because planar and cylindrical surfaces make up the largest number of geometric surfaces required for high performance mechanical components.

2 Background

The DASH process starts with a computer-aided design (CAD) model, which is converted into the Additive Manufacturing File format with extensions for Tolerances (AMF-TOL) through the AMF Creator software developed by Srinivasan (2014). This format is like the normal additive manufacturing file (AMF) format but with the expanded capabilities to include geometric dimensioning and tolerancing (GD&T) (LEADRP, 2022; FARO, 2023) information directly in the file.

Within AMF Creator, the user can specify critical features, material conditions, datum and tolerances associated with each feature and save this information directly into the AMF-TOL file. Then, using the information about critical features, visibility analysis is performed (Chen et al., 2018), and sacrificial support structures are added to fixture components in such a way to allow machining of critical features without interference. The AMF-TOL file is updated to include these support structures, and machining allowances can be automatically generated to ensure there is enough material to remove during machining (Srinivasan, 2014). Once this file has support structure and machining allowance, the part can be printed using any AM method.

After the parts have been printed and removed from the build platform, they can be placed into the

two rotational jaws (4th axis) of the milling machine. Here, a laser scanner is used to localize the part, and collect data to determine how much additional material is remaining on the part itself. Using the scan data, a transformation matrix is created to align the original CAD model with the physical part location in the machine. Then, toolpaths are automatically generated using a MasterCAM plugin (Mastercam, 2021) which can be uploaded into the milling machine for whole model roughing and final finishing of the critically marked surfaces. Figure 1 shows the DASH process sequence.

When a part is detailed in a CAD model, the part coordinates and related Datum are identified for the part. The standard for machining is to locate the part on the machine making the part coordinate system align with the machine axes. Unfortunately for parts that have many contoured surfaces or for parts that need alternate orientations to facilitate machining access (as shown in Figures 1–3), the part coordinate system needs to be translated to the orientation and presentation noted in Figure 3. This makes machining the part feasible. That is, the machine is capable of the required kinematics to access all surfaces that require machined tolerance. We do not include "tolerance stacking" in this paper, but the standard methods used to satisfy the tolerance limits can be used. That is beyond the scope of this work. Offsets are used to shift location of parts that are aligned parallel to the machine axes. The alignment for these methods is performed automatically in related literature (Yang et al., 2011, 2009; Frank et al., 2005, 2006; Yang et al., 2012; Srinivasan et al., 2015a,b).

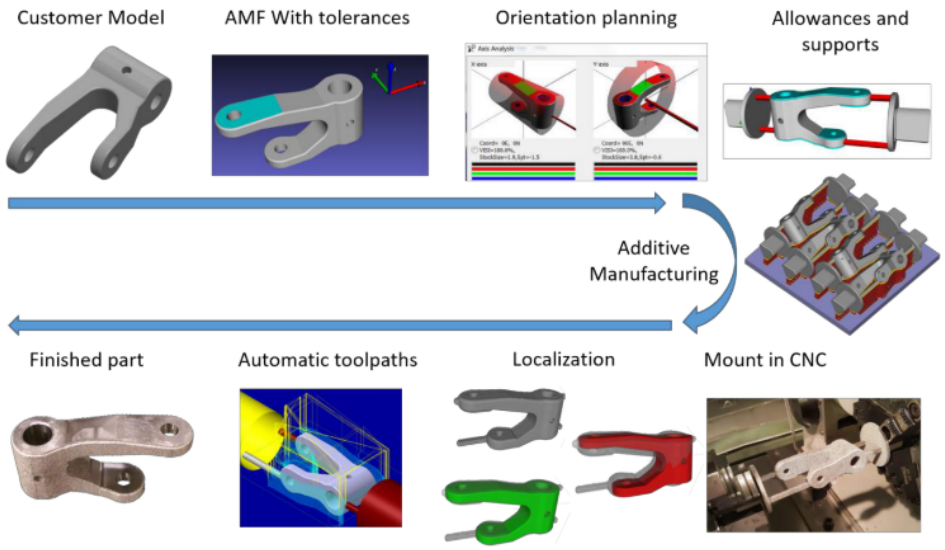

Figure 1: DASH process sequence (Srinivasan, 2014).

In terms of being able to measure tolerance for circles and cylinders, Traband et al. (2004) discuss a statistical approach using point sampling, specifically for Coordinate Measuring Machines (CMM), but their method can directly be applied to OMM with a probe since it is a similar process. A nonlinear regression model is used to represent a cylinder in terms of five parameters of interest shown in Table 1. Equation (3) provides the Gauss-Newton nonlinear least squares regression model. Error terms, ε_i, are assumed independent and normally distributed. Sample radii measurements are represented by r_i.

Let

$$\gamma = C' \cos\phi' - C\cos\phi, \tag{1}$$
$$\delta = C' \sin\phi' - C\sin\phi, \tag{2}$$

Table 1: Parameters to estimate using nonlinear regression model in Equation (3) (Traband et al., 2004).

Parameter	Description
R	Radius of Cylinder
C	Eccentricity
	(distance from nominal center to center of fitted cylinder)
ϕ	Eccentricity Angle
C'	Eccentricity at Z_{max}
ϕ'	Eccentricity Angle at Z_{max}

then

$$\begin{aligned} r_i &= C\cos(\theta_i - \phi) + \gamma\frac{z_i}{z_{max}}\cos\theta_i + \delta\frac{z_i}{z_{max}}\cos\theta_i \\ &+ \sqrt{R^2 - \left[C\sin(\theta_i - \phi) + \gamma\frac{z_i}{z_{max}}\sin\theta_i - \delta\frac{z_i}{z_{max}}\sin\theta_i\right]^2} + \varepsilon_i. \end{aligned} \tag{3}$$

Nonlinear regression provides the opportunity to make statistical inferences on tolerances based on model parameters and avoids errors in linear models (Traband et al., 2004). The regression model produces estimates for the parameters in Table 1 stored in a matrix denoted **Q**. These can be used to develop decision rules to accept or reject parts with respect to size and position tolerance of cylindrical features. Refer to Traband et al. (2004) and Kelly (2018) for implementation details.

The rest of the paper is organized as follows: Section 3 outlines the methodology for parameter estimation, Section 4 summarizes an experiment applying the model to a DASH-created sample part, Section 5 provides an economic cost evaluation, Section 6 summarizes guidelines for OMM sampling, and Section 7 gives some closing thoughts.

3 Methodology

3.1 Machine Localization

A unique characteristic of the AMF-TOL file format created for the DASH process is the capability to incorporate "features" and "associated tolerances" directly into the file (Srinivasan, 2014). Tolerances are an integral part of any manufacturing process and provide an allowable deviation from specified feature sizes or locations. The basis for the AMF-TOL format is extensible markup language (XML) which makes the information within easily accessible.

Due to the complex geometries associated with AM parts, physically probing three different planes as datum is not always a possibility. For this reason, the datum used to determine position of features will be the origin of the part with respect to the machine. This origin is determined using the FARO scanner (FARO, 2019) and is limited by the precision of this measurement device. Although no physical contact to detect datum features occurs, the accuracy of the FARO scanner was verified by Srinivasan (2014) and is adequate for generating toolpaths to machine metal components. For these reasons, position determination of features is still valid through this measurement method.

Initial user defined feature information is specified with respect to the origin of the original CAD file before support structures are added and before the origin is relocated for machining toolpaths to be created. However, as transformations occur for sacrificial support placement and registration of the part within the CNC machine using a FARO scanner, the metadata and location of critical features can also be transformed, meaning that the true location of these features are known in the machine after scanning (within the limits of the scanner). Figure 2 shows origin transformations through the process.

Transformation information is stored in transformation matrices, which the DASH process utilizes to automatically generate toolpaths for specific features on AM parts. We will utilize the same information to determine the expected size and position of features in the CNC machine so probing paths can be automatically generated.

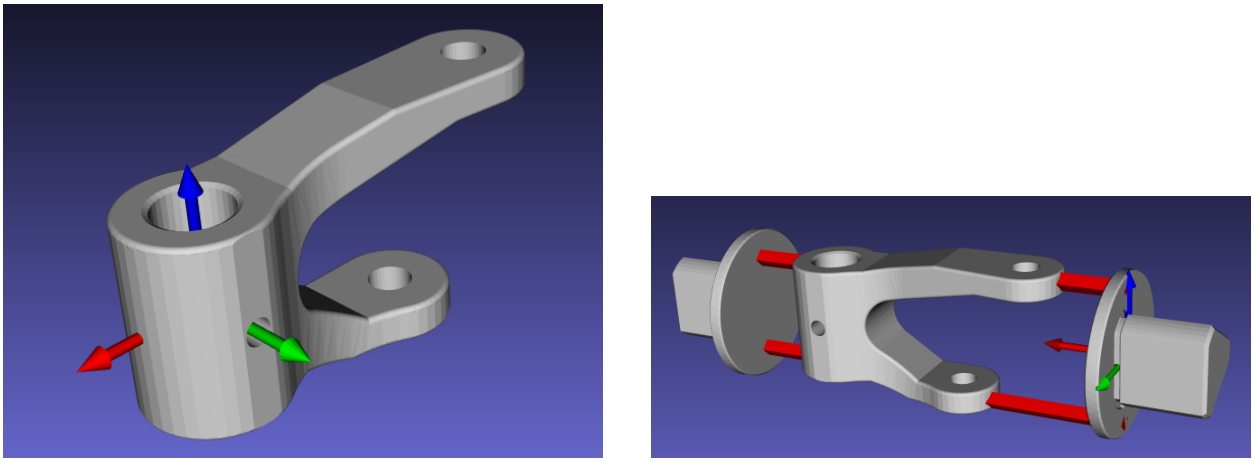

(a) (b)

Figure 2: (Color online) (a) Original part coordinate system origin as defined on a CAD system. (b) Relocated part coordinate system with highlighted (red defining primary rotation plane) after sacrificial supports are added to the part.

Because information for transformations, feature location, size, and tolerance callouts are accessible in the existing DASH files. These values can automatically be extracted and utilized to create probing toolpaths using a variety of programming languages to open and read information from files. A Python script was developed to automatically extract feature location information to be used for probing path generation.

3.2 Probing Point Selection Strategy

When pre-determining probing point selection strategy it is important to balance the need for adequate sample information with the time it will take to collect additional data points. Because of this, the points must be spread out in a strategic way. Some strategies suggest a uniform or "bird-cage" strategy to determine sample points (Janecki et al., 2015). However, certain flaws in CNC machining may follow a similar repeating pattern and could be missed. Taking a random sample of points might mitigate this symmetric problem; however, this creates the possibility that all or many of the points are grouped very closely together. This could create large open gaps in the sampling spread, allowing for certain defects to occur in between samples. There must be a balance between an increased number of sample points for accuracy and increased time and cost associated with the sampling of the points.

To measure a cylinder for cylindricity and position, we must take sample measurements of the size of the feature at more than one position along the central axis of the cylinder. Since traditional milling machines are only capable of drilling along the Z axis, we will call these Z heights. Measurements at multiple Z heights must be taken to ensure alignment of the feature with the drilling or probing axis.

At each Z height, we assume that the cylindrical feature axis is in line with the Z axis of the machine. Therefore, we can consider probing movements in the XY plane at different angles from the $+X$ axis as $0°$. This is consistent with the inputs required for Renishaw probing commands which measure angles from the $+X$ axis as $0°$. Probe radius measurements will only occur in the XY plane once it has reached a valid Z height.

To create a uniformly distributed "bird-cage" sampling pattern, the first measured angle would need to occur at the same angle for each Z height. This would ensure that all other measurements happen at the same angles at every Z height. However, this is not the only method considered because we could choose to take different angular measurements at each Z height.

To determine an appropriate probing strategy, seven different sampling methods were considered. The seven sampling methods were different in the way they: (1) select heights along the cylinder axis (Z axis), (2) select angles to measure at each height, and (3) choose the first angle to probe at each Z height. For example, it is possible that the angles at each Z height are uniformly distributed between $0°$and $360°$, but the first

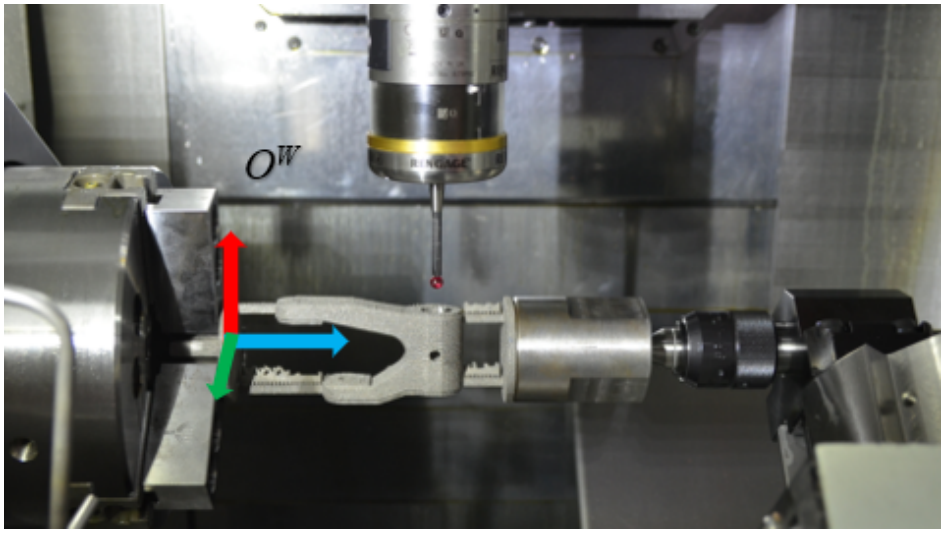

Figure 3: (Color online) Part mounted in CNC machine after final transformation. Workpiece origin is denoted by arrows and designated as O^W.

angle probed is different at each Z height (e.g. $Z_1 = 0.5$ and angles $\in \{0°, 90°, 180°, 270°\}$ but $Z_2 = 0.25$ and angles $\in \{45°, 135°, 225°, 315°\}$). Table 2 describes the method used for each sampling strategy.

Table 2: Sampling methods distinguished by selection of Z height, angle, and first angle. See the Appendix for additional illustrations.

Sample Method	Z Heights	Angles	1st Angle
M1	Uniform	Uniform	Random
M2 (bird cage)	Uniform	Uniform	Identical
M3	Uniform	Random	Random
M4	Random	Uniform	Random
M5	Random	Uniform	Identical
M6 (random)	Random	Random	Random
M7 (spiral)	Uniform	Uniform	Uniform

Methods M1–M6 all employ multiple sample radii taken at each Z height and a minimum of two Z heights to measure cylindricity. However, M7 creates a spiral pattern over the depth of the bore. One sample radius is taken at each height, and the angles and Z heights uniformly change to span the length of the hole depending on the number of sample points taken. Figure 4–5 (and Figure 11–15 in the Appendix) illustrate how sample points are spread out for the various methods with (red) dots indicating probing locations. These seven sampling strategies were considered by measuring a cylindrical feature on a DASH process created part. Probing paths were automatically generated for each method.

3.3 Probing Path Generation

Renishaw Inspection Plus software is installed onto a machine when a Renishaw touch probe is set up on any CNC machine (Renishaw, 2008). The probe and software combination are most directly suited for setup and fixturing parts but does provide some basic measurement capabilities. Other probing and measurement software exist to perform more detailed analysis of part size, but these can be very expensive.

Single point measurement cycles are an effective method to collect data of size, position and direction of position error. Traditionally single point measurements are used only to measure along the X, Y, or Z axis for quick setup and location of a part. The Renishaw Inspection Plus software does provide the option

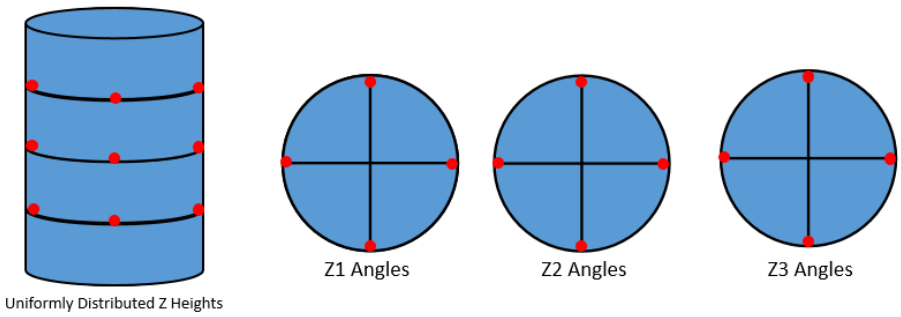

Figure 4: Method M2 sampling strategy known as the"bird-cage" method. Uniform Z height distribution and uniform angle distribution with same first angle at each Z height.

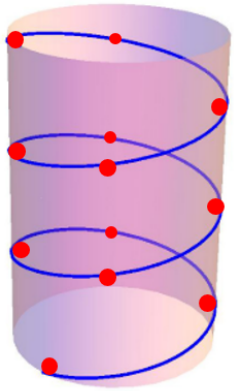

Figure 5: Method M7 sampling strategy (helix adapted from Lăzureanu (2014)).

to run an "Angle single surface measurement" cycle (O9821) which measures the distance from the starting point of the probe to the surface of a part in any direction in the XY plane. Measurements at many angles can be used to determine not only the size of a feature, but the true position error and the direction the error has occurred in.

Knowing the sample radius size and direction of probing sample from the generated numerical control (NC) code, we can export the updated values to a computer using a machine specific print statement (DPRINT) on the Haas VF3 (Haas, 2019). Since the VF3 has limited interface and computational power without additional software, a separate computer is used for mathematical computations regarding best fit and tolerances. A laptop equipped with a terminal emulator software (PuTTY) (Tatham, 2021) is connected to the VF3 directly through a serial port RS-232 connection. By placing DPRNT commands directly into the probing NC code, we can instantly extract measurement information from the CNC to the laptop. To make code generation easier, all measurement values (#188) are saved to a unique and vacant macro variable. Then, all variables are printed to a text file or external computer at the end of the entire probing cycle. This information can be saved into a text (.txt) file and imported into Microsoft Excel for easy calculations. The interested reader can consult the Appendix or Kelly (2018) for more technical implementation details.

3.3.1 Visual Basic for Applications (VBA) Code Generation

Visual Basic for Applications (VBA) code was written to automatically generate probing toolpaths for the multiple sampling strategies discussed above (M1–M7). The input required to successfully generate includes:

1. Rotational angle to align the cylindrical feature with the Z axis (tool),
2. X Center location of the cylindrical feature,
3. Y Center location of the cylindrical feature,
4. Max Z of cylinder,
5. Nominal Diameter of Bore,
6. Bore Total Depth,
7. Number of Angles to measure per Z height,
8. Number of Z heights to measure,
9. Through hole as Boolean.

As discussed earlier, these values come directly from the AMF-TOL file and can be automatically populated into Excel.

3.3.2 Collision Considerations

Since the probing strategy for this research is intended only for cylindrical features, a safe approach path is predictable, which allows us to avoid unwanted collisions between the probe and machine. Certain common and predictable types of collisions and safeguards against these situations are discussed in this section.

First, the probe stylus contains a spherical tip, cylindrical shaft, then a conical taper which is wider than the shaft. If the probe does not make contact on the edge of the spherical ruby tip, the measurement information would be incorrect. To prevent any issue with this, the maximum depth of the bore feature must be smaller than the length of the shaft. This will ensure the probe does not move too far into the hole for an invalid measurement or a potential collision with the probe body. Similarly, the maximum Z height for a probing sample is designed to occur 0.64mm (0.025") below the max height of the machined hole.

Second, measurements in the XY plane are designed to occur on the radius of the spherical probe tip. For blind holes, it is important to make sure that the tip of the probe does not make contact in the Z direction before the actual measurement cycle will occur. To prevent this, the minimum Z height that the probing cycle will generate is offset from the lower wall of the pocket by the radius of the probe tip plus 0.25mm (0.01") for additional buffer. Similarly, the maximum Z height for measurement is reduced by the

probe tip radius plus an additional 0.25mm (0.01") to ensure that contact will always happen on the true outer edge of the probe. If the maximum Z height determined by the AMF file was used, a probing cycle at that height would not make contact on the edge of the probe tip and report incorrect measurement values.

Third, the diameter of the hole to be measured must be greater than the diameter of the probe tip. A constraint was added to the nominal hole diameter requiring this value to be greater than 6.10mm (0.24"), the diameter of the probe tip.

Finally, it is possible that the stylus of the probe completely avoids any sort of collision which would trigger the safe move alarm, but the body of the probe does interfere with the machine or workpiece. The body of the probe is significantly wider than the stylus and would not detect a collision without the stylus first making contact. To avoid this problem, an alarm was added which alerts the user of a potential collision if the X center location of the hole is less than the radius of the probe body plus the width of probe jaws. This safeguard was only created as an alarm because there are circumstances when probing could successfully occur without collision when the probe is outside the "safe" range of X values. For example, depending on the rotational orientation of the part, the three chuck jaws could be in significantly different positions. If the probe measurement were to occur in between two chuck jaws, the tool could move significantly closer to the chuck face without collision.

3.3.3 Toolpath Code

The overall process for probing toolpath generation follows the process described in Figure 6, starting after the tool has been called into the spindle. This process will work for collecting sample measurements for the size and location of bores created on a CNC machine. First, the probing tool is called into the spindle. Then the part is rotated to the proper orientation to align the bore's central axis with the tool. Next, the probe is turned on before any movement occurs. Safe X and Y movements happen simultaneously to align the probe stylus with the main shaft of the bore significantly higher than the part in the machine. Only after this will the probe perform a safe move to approach the part along the Z axis. It should be noted that X and Y movements, or rotational 4th axis movements only occur while the probe is significantly higher than the part, in the tool change position Z height. The approach move in Z only occurs once the probe is above the center of the hole. The probe should move directly into the hole center avoiding any unwanted collisions. However, since we only travel using safe moves, any unwanted interference with the probe stylus will trigger and alarm, informing the user that there is some problem with the location or size of the hole. Probe sampling occurs at every angle determined at each Z height. Safe Z movements and angle sampling can be repeated to meet the needs of any combination of sample points. Once probing measurements are complete, a safe Z move raises the probe out of the way to a safe height above the part. If there are more holes, this process can be repeated. After all sampling is complete, the probe is shut off to extend battery life.

3.4 Computation for Best Fit, Size and Position

To evaluate size and/or position of the cylindrical features sampled with the probe, the Gauss-Newton nonlinear least squares method described in Traband et al. (2004) is applied. This method iteratively finds the best fit of measured radius and center location by minimizing the sum of squares error (SSE) and updating the parameter estimates stored in $\mathbf{Q}$ until acceptance criterion are met (Traband et al., 2004). Refer to Table 1 for definitions of the five parameters of interest.

The process begins with an initial guess of the parameter values, denoted $\mathbf{Q}_0$. The initial radius is populated with the first sample radius value, and the other parameters are arbitrarily assigned initial starting values not equal to zero and not equal to one another.

VBA code executes this the Gauss-Newton nonlinear least squares regression algorithm to solve for the parameter values in $\mathbf{Q}$. This is an iterative process which continues until the SSE or the difference between SSE in two consecutive iterations is significantly small. To converge, SSE must be less than 0.000001 or the difference must be less than 0.00001. Through testing of the code, it was determined that these values were quickly obtainable and provided more than enough accuracy with respect to CNC machine capabilities. The CNC machine used for this research is accurate to 0.0025mm (0.0001") and therefore the convergence criteria is at least one order of magnitude greater than the machine capabilities. This process generally requires only

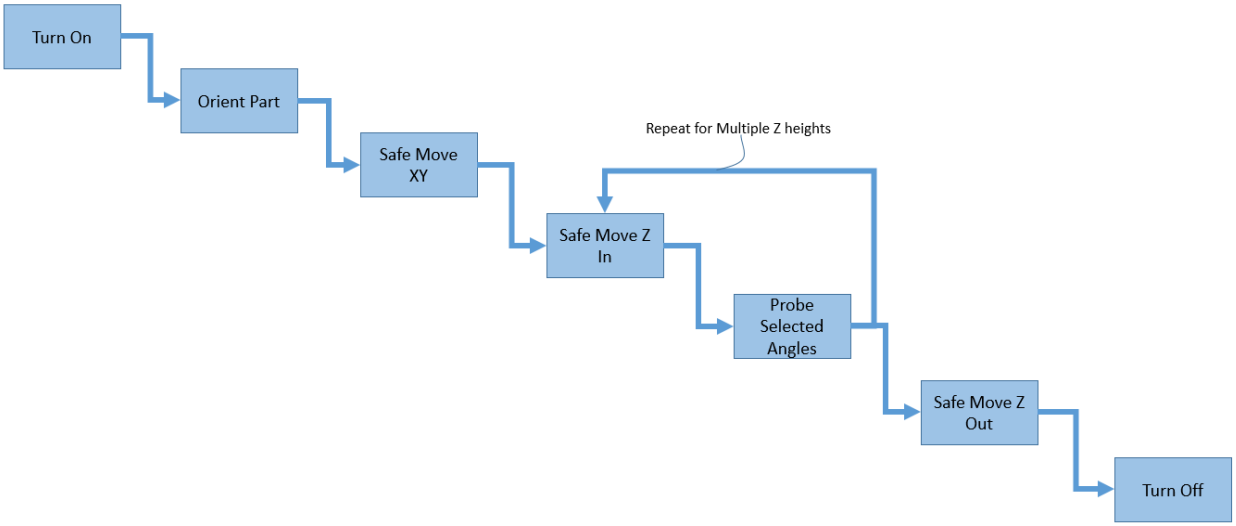

Figure 6: Process flow chart describing the order of events for probing toolpaths.

a few iterations before a confidently small SSE is determined, but it is possible that the regression does not ever converge depending on the initial starting parameters (Traband et al., 2004). If this occurs, simply changing initial parameter values and restarting works well in practice. Once the acceptance criteria is met, best fit parameters have been calculated.

After parameter estimates have been calculated, we can develop confidence intervals around these parameters to determine their accuracy. Kelly (2018) provides the procedure to compute the variance-covariance matrix $\mathbf{V}$ to determine confidence intervals are around the parameter estimates R, C, ϕ, C', and ϕ'. The values from the main diagonal of the $\mathbf{V}$ matrix correspond to the variance of each parameter which will be used to construct confidence intervals. Confidence interval (CI) calculations are slightly different for size, position, and material condition. The interested reader may consult Kelly (2018) for implementation details.

3.5 Sampling Strategy Evaluation

To determine the accuracy of each sample strategy, a part was created through the DASH process and inspected using the seven different sampling strategies discussed above. For each sample strategy, multiple probing cycles were run with varying amounts of sample points. Total number of sample points per cycle varied from 12 to 60. Also, the total number of samples per Z height, and the total number of Z heights were varied to emulate many different sampling strategies.

The range of the confidence interval around R, C, and C' was determined for each sample run across all sampling strategies. Each test was run with 90% confidence (chosen arbitrarily) for both size and position with respect to a RFS callout. JMP statistical software (SAS, 2019) was used to determine if there were statistically significant differences in the mean confidence interval range around the measured radius (R), eccentricity (C) and eccentricity at Z_{max} (C'), as well as to determine the variance in each sampling strategy.

First, data normality was verified using normal quantile plots. Observed R, C, and C' values were all normally distributed. Also, the confidence interval range for R, C, and C' were verified to be normally distributed. This is expected because of the large number of samples collected across the multiple methods tested.

Next, Tukey-Kramer pairwise testing (Tukey, 1949; Kramer, 1956) was used to determine which sampling strategies were significantly different than the others. The Tukey-Kramer test showed that Methods M4 and M7 had statistically significant difference in mean value observed for confidence interval range for R, C, and C'.

JMP was then used to show that variances between the seven strategies were also statistically significantly different. Both Bartlett's and Levene's tests for equal variances show that methods M4 and M7 have signif-

icantly higher variance than the other methods in confidence interval size for R and C'. Levene's test shows that Method M4 is significantly different with regard to parameter C. Since the mean confidence interval for all three parameters of interest is significantly larger for methods M4 and M7, it is not recommended to use these strategies. Also, our finding that the variance in confidence interval size is significantly different for at least two out of three parameters of interest further supports the recommendation not to use methods M4 or M7.

Finally, the process was repeated considering only the methods which were not previously determined to be statistically significantly different. This includes methods M1, M2, M3, M5, and M6. Tukey pairwise testing could not detect a significant difference in means between confidence interval size for R or C'. However, Tukey's test did detect a significant difference between method M1 and M2, the largest confidence interval size, and smallest size respectively.

Levene's test for equal variances shows a significantly larger variation in confidence interval range around R for Method M6 and around C parameter estimate in method M1. There was no significant difference in variation between any pair for the confidence interval range around parameter C'.

Because of the results of the Tukey's test and Levene's test for equal variance around C confidence interval size, it is recommended not to use method M1 as a sampling strategy for measurement. However, we cannot conclude that there is significant difference between sampling strategies M2, M3, M5, or M6.

Through testing, we have shown that methods M2, M3, M5, and M6 perform similarly in measuring feature size. However, there are some inherent risks associated with each method which should be considered when selecting probing strategy. Since method M2 uniformly distributes sample points, it is possible that each probing point could correspond directly to a repetitive defect around the feature. Should symmetrical deviants occur at equal intervals around the feature, the bird-cage method may incorrectly detect parameter information. Simple visual inspection of the part may lead an inspector to suspect a symmetric defect, such as a vibration defect, around the profile of a cylinder. If a repetitive defect is suspected, the bird-cage method should not be used, or sample angles should be more closely investigated before measurement.

Method M6 is completely randomized and runs the risk of grouping all points very close together, inaccurately collecting data on the part. Should all sampling points randomly be assigned to one small area on a feature, defects in other areas may not be detected. Due to the risk of inconsistency in completely random sampling, it is not recommended to use method M6.

For further measurements as part of this work, the bird-cage method was utilized. After visual inspection, there was no reason to believe that a recurring defect was present. JMP results also show that the overall variance and mean confidence interval size calculated from sample measurements was minimized with method M2. The bird-cage sampling strategy for cylindricity is also one valid procedure defined ISO-12180 (Janecki et al., 2015). We will now further investigate the number and distribution of sample measurements across the Z heights and circumference of the part.

3.6 Number of Sample Point Evaluation

To validate the accuracy and efficiency of this inspection system using the birdcage method, a cylindrical bore was created in an aluminum piece of bar stock with nominal diameter 12.7mm (0.5"). From thorough manual inspection, we know the true diameter of this cylinder to be between 12.70mm (0.500") and 12.78mm (0.503"). The birdcage sampling strategy was then utilized to take sample points of this bore and create confidence intervals around the true size and position of this feature. From preliminary data to determine the optimal sampling strategy and results from the experiments presented in Traband et al. (2004), it is clear that less than 20 sample points will not provide enough information to create narrow confidence bounds around the estimated parameters of interest. Both tactile and laser methods are commonly used in-situ to inspect mechanical workpieces. Both of these methods are capable of generating thousands of data points in a few seconds. For this paper, an older touch probe was used and programmed manually to gather points from a broad section of the cylindrical surface. We started with 20 sample points to see what kind of statistical confidence could be garnered from a quick manual gathering of data. When this system is automated, a large number of surface points could be quickly collected. The study was to see approximately how many data points would be typically needed for a confident response. We also looked to see if the pattern of point selection would affect the measurements.

Results from these experiments show that the range of the confidence interval surrounding the parameters

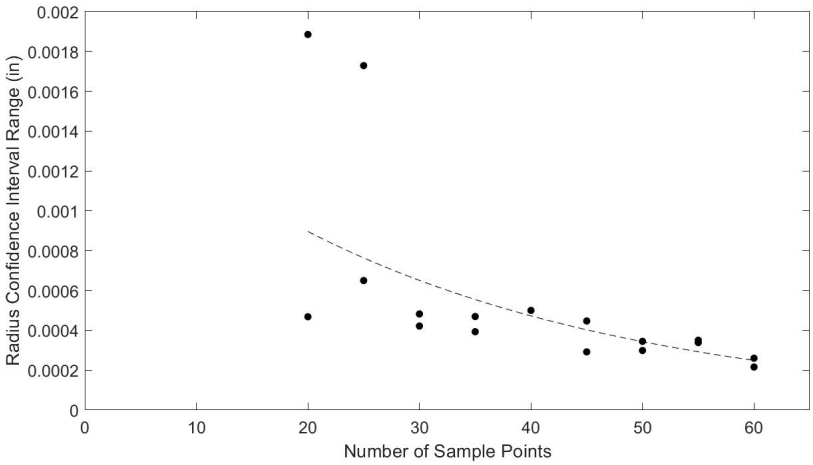

Figure 7: Confidence interval range surrounding the estimated R parameter with 90% confidence.

of interest decrease exponentially, eventually converging on an approximate value. This tells us that we have diminishing returns on the value of taking additional sample points. Figure 7 shows that as the number of sample points increases, the change in the size of confidence interval estimate decreases. It appears that the 90% confidence interval regarding the true radius of the machined bore converges at approximately 0.0051mm (0.0002"). After just 30 sample points, the predicted range around the radius is less than 0.0127mm (0.0005"). Again 90% confidence was chosen arbitrarily but could easily be recalculated with another level of confidence.

We can see similar patterns in Figure 8 which shows the changes in confidence interval range regarding C and C' parameters as sample size increases. Both show drastic variation reductions after 25 sample points which suggest convergence at approximately 0.00381mm (0.00015") and 0.00178mm (0.00007") for C and C' respectively.

The confidence intervals surrounding R, C, and C' all converge with values less than 0.025mm (0.001"). This level of accuracy is sufficient to make judgements about tolerance verification for cylindrical features.

The time of the probing cycle depends primarily on the number of sample points measured. Location of points and type of probing cycle did not affect the overall time to complete probing. Figure 9 shows a linear relationship between the number of sample points and the time to complete the probing operations. We see a Y intercept of approximately 31 seconds, which accounts for the tool change to get the probe and machine movement to the location of the first probing point which occurs at the beginning of each probing cycle. Once a Renishaw probing macro is called, the feed rate of the machine is fixed based on the feed rate established within the macro. After this initial tool change and probe movement to the part, we see that the time to complete probing is approximately 3 seconds per sample point.

3.7 Recommendations

From our "on machine" experiments, it appears that parameter estimates are very accurate after approximately 30 sample points. We recommend that this should be set as the minimum required number of sample points to accurately measure a cylindrical feature. Additional sample points (especially for systems equipped with a DASH-like software system) can be taken to further decrease the size of the confidence interval surrounding parameter estimates for minimal cost. It should be noted that for a manual system, the cost of consuming additional machine time and programming these features needs to be carefully analyzed. The DASH process was designed to provide an efficient way to produce custom or legacy components.

As an initial starting point, it is recommended that taking 40–50 sample points, distributed using the birdcage method described above should be used. For unique one-of-a-kind components, combining production and inspection within a single machine should generally save on setting up multi-use inspection equipment time and money. Our early experimentation shows that a touch probe is capable of accurately

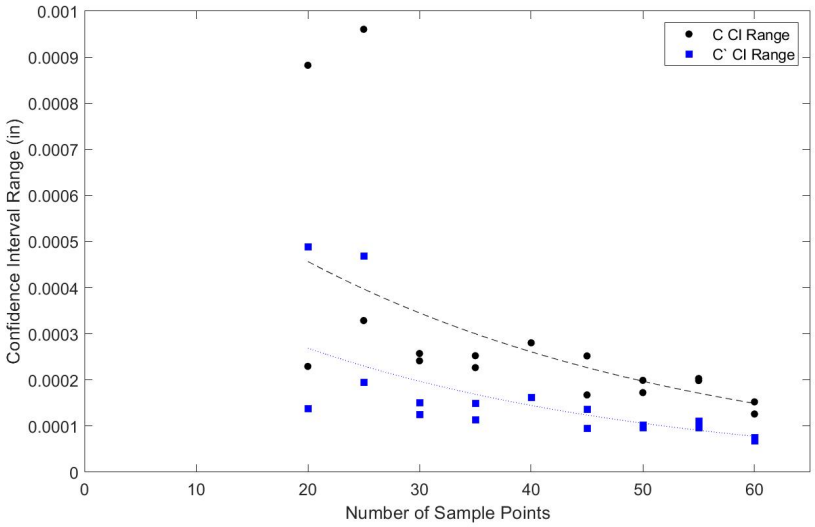

Figure 8: (Color online) One sided confidence interval range surrounding the estimated C and C' parameters using 90% confidence and Maximum Material Condition (MMC).

Table 3: Product specifications for the part measured in this experiment in the format required by the software used in this study. Values were expressed using the AMF-TOL file for the part shown in Figure 2.

Primary Shaft Details	Value
Central Axis Vector	[0.00, 0.00, -1.00]
Centroid	[0.00, 0.00, 0.00]
Depth	34.889mm (1.3736")
Cylinder Top (Z position)	17.4458mm (0.686842")
Diameter (nominal)	14.0726mm (0.554040")
Through Hole	True
Cylindricity Call-out	$\pm$ 0.127mm (0.005")
Position Call-out (Material condition)	$\pm$ 0.127mm (0.005") (MMC)

and automatically measuring cylindrical features.

4 Case Study & Experimentation

4.1 DASH Created Bracket

To measure the effectiveness of this sampling strategy a part was created through the DASH process. Refer to Figure 2 to see this bracket with one main cylindrical bore labeled as the "Primary Shaft". During Phase 1 of the DASH process, metadata was extracted for this part feature and then collected to determine the nominal diameter, location, and depth of hole. Tolerance information was also extracted from the AMF-TOL file. All information for this feature is described in Table 3.

Continuing through the DASH process, sacrificial supports were added, and corresponding transformation values were updated to reflect the part's translation and rotation. The part was then additively manufactured in titanium using an electron beam melting process. Next the part was mounted into a Mazak Integrex i 100 (Mazak, 2019) as shown in Figure 3. A FARO EDGE scanner equipped with a laser scanning head was used to localize the printed part to the CNC machine and update the transformation information per DASH protocol. Complete transformation information from the initial AMF-TOL file ori-

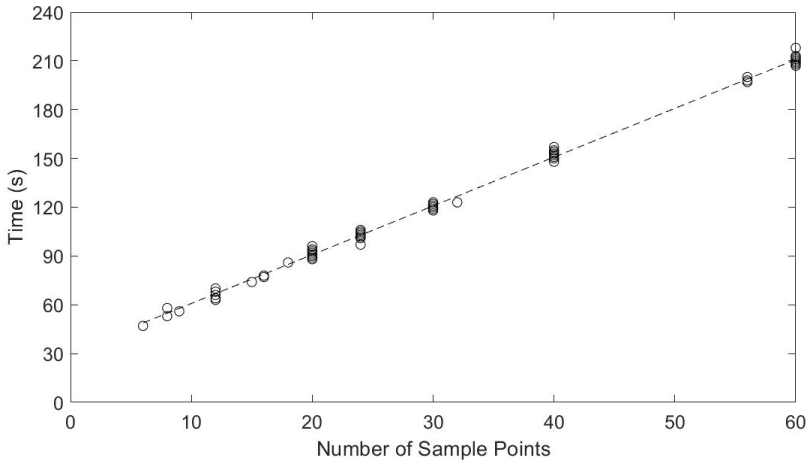

Figure 9: Relationship between time to probe and number of sample points. Fitted line $Time = 2.9994 NumPoints + 30.829$ shown for visualization ($R^2 = 0.9982$).

Table 4: Transformation information to align virtual CAD model with physical part location in the machine.

Description	Values
Transformation Vector $< x, y, z >$	$< 5.04055, -0.00129, -0.00376 >$
Rotation about X Axis	$134.9184°$
Rotation about Y Axis	$0.00°$
Rotation about Z Axis	$0.00°$

entation to the final machine orientation was calculated using the information in the transformation ".xml" file created. Table 4 lists final transformation values.

Transformation and primary shaft feature information were combined to determine the expected size and position of the cylindrical feature after machining. Machining toolpaths were created to circle interpolate the bore of the primary shaft.

Probing toolpaths were automatically generated using VBA and the required inputs described above. Locations for 40 sample points were determined using the birdcage method and sampling strategy relating to this work. Eight different angles were measured over five different Z heights. After machining the part, the probing cycle was run to measure the cylindricity and position of the primary shaft. Sample radii measurements using the RMP-600 probe (Renishaw, 2023) were recorded as macro variables within the Mazak and then transferred to an external computer to be used for calculations.

The probing cycle took 2 minutes and 32 seconds to complete, including time for a tool change. Passing the data through the VBA algorithm only took a few seconds and the parameters of interest were calculated as:

$$\begin{aligned} R &= 6.8966\text{mm } (0.27152"), \\ C &= 0.3734\text{mm } (0.0147"), \\ \phi &= 3.477 \text{ radians}, \\ C' &= 4.5347\text{mm } (0.17853"), \text{ and} \\ \phi' &= 3.2978 \text{ radians}. \end{aligned}$$

Since the magnitude of C and C' both exceed the given position tolerance requirement of $\pm$ 0.127mm (0.005") Maximum Material Condition (MMC), the part would be unacceptable. The position of this feature is outside

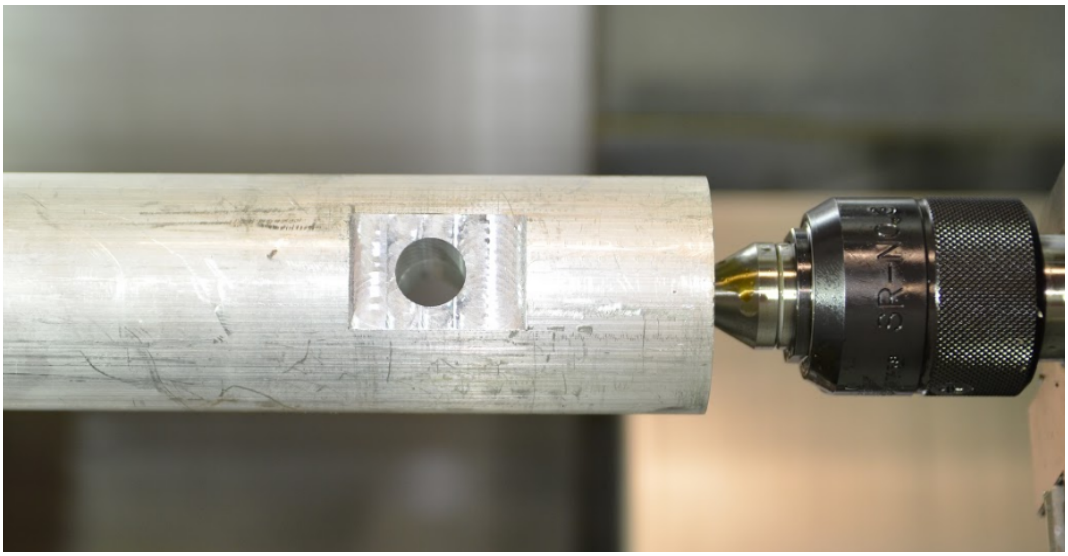

Figure 10: Cylindrical bore manually machined out of aluminum bar stock.

tolerance specifications. Creating 90% confidence intervals around the parameters:

$$\begin{aligned} \text{90\% CI for } R &= [6.79618,\ 6.99709]\text{mm } ([0.267566,\ 0.275476]\text{"}), \\ \text{upper bound for } C &= 0.4741\text{mm } (0.0186657\text{"}), \\ \text{upper bound for } C' &= 0.510438\text{mm } (0.020096\text{"}), \text{ and} \\ \text{Diameter} &= [13.5924,\ 13.9942]\text{mm } ([0.535132,\ 0.550952]\text{"}). \end{aligned}$$

The confidence interval for diameter does not include the nominal value for the diameter. Also, the lower bound on the confidence interval falls outside the acceptable range of values for which the feature could be accepted, which means that we cannot be confident that the feature is accurately machined. Further analysis shows that the range of values that the confidence interval takes on is 0.2007mm (0.0079") on the radius and therefore 0.4013mm (0.0158") on the diameter. This far exceeds the tolerance callout of ± 0.127mm (0.005") for cylindricity. We cannot be confident that this part is within tolerance specifications. Again, we would fail to accept that the feature created was within tolerance with respect to cylindricity.

Manual inspection of this part also verified that the feature was improperly machined and does not fall within tolerance specifications. Manual measurements of the bore diameter ranged from 13.2mm (0.521") to 14.4mm (0.565"). This difference of 1.12mm (0.044") is significantly greater than the allowable tolerance for this feature. Since the size of this part is unacceptable, we reject the part and do not need to continue to measure the position accuracy.

4.2 Accurate Bore

To validate the effectiveness of this inspection system, a cylindrical bore was carefully created in a piece of aluminum bar stock. Figure 10 shows this cylindrical bore.

The nominal diameter for this piece was 12.7mm (0.500") with cylindricity callout of ± 0.127mm (0.005") and position callout of ± 0.127mm (0.005") MMC. Since this part was not created using the DASH method, feature location information was manually entered into a userform so that automatic probing paths could be created. Again, 40 sample points were taken over 5 different Z heights using the birdcage strategy as recommended.

Results from the VBA algorithm show the estimates for parameters of interest as follows:

$$\begin{aligned} R &= 6.37771\text{mm } (0.251091\text{”}), \\ C &= 0.03861\text{mm } (0.00152\text{”}), \\ \phi &= 1.815705 \text{ radians}, \\ C' &= 0.02896\text{mm } (0.00114\text{”}), \text{ and} \\ \phi' &= 4.57937 \text{ radians}, \end{aligned}$$

with 90% confidence intervals:

$$\begin{aligned} \text{90\% CI for } R &= [6.37136,\ 6.38406]\text{mm } ([0.250841,\ 0.251341]\text{”}), \\ \text{upper bound for } C &= 0.0457\text{mm } (0.0018\text{”}), \\ \text{upper bound for } C' &= 0.0330\text{mm } (0.0013\text{”}), \text{ and} \\ \text{Diameter} &= [12.743,\ 12.768]\text{mm } ([0.50168,\ 0.50268]\text{”}). \end{aligned}$$

All values within the confidence interval fall within the acceptable ranges of values that this part can take on [12.6, 12.8]mm ([0.495, 0.505]”). For this reason, we would choose to accept that the feature is the correct size. Confidence intervals around the true position of this feature do not exceed 0.127mm (0.005”) as specified in the AMF-TOL. For these reasons we can accept the accuracy of this machined feature.

Manual inspection of this cylindrical feature confirmed the results of the probing strategy. Manual measurement of the bore diameter ranged from 12.7mm (0.500”) to 12.8mm (0.503”), falling within the acceptable tolerance range for size. To verify position accuracy, the part was placed into a different machine and the origin was manually set. Then, a 12.6mm (0.495”) pin GO gauge was moved to the nominal location of the bore and successfully passed through the feature. Since there was no collision, we can accept the feature's location accuracy.

Results from this study show that these inspection guidelines and probing system can detect a bad feature as well as an acceptable feature. The guidelines discussed in Section 2 were successful in measuring the accuracy of a cylindrical bore and can be utilized to make decisions for tolerance evaluation.

5 Economic Cost Evaluation

5.1 Production Quantity

Production environments would often want the CNC machine to be actively utilized as much as possible, with little down time. For this reason, part inspection and qualification usually occur off the CNC machine manually or on a CMM. This is even more common in high volume production settings where the parts are low cost. Only a sample of parts will be inspected, and the cost of a bad part is relatively low. For this reason, it makes sense to continue machining, and simply scrap the low-cost, high-volume products.

The fundamental difference between DASH and traditional production processes is the intended production quantity. DASH is designed for very low production runs of highly customized, low volume parts such as legacy components. The generally slow nature and high unit cost for AM metal parts is best suited for low volume production of customized components. The unit cost for a Ti64 additively manufactured bracket is estimated to be approximately $1200 per unit compared to only $400 per unit if created by forging (Laureijs et al., 2017). This bracket is a good representation of an average part that may be produced through the DASH process and can therefore be used as a basis for calculations. Since we expect the accuracy of features to be important and the total production run to be small, the best solution is to automatically measure the parts while they are still fixtured in the CNC. This may also allow the opportunity to re-machine any areas with excess material before the part is completely removed from the machine. When possible, rework is expected to be significantly cheaper than scrapping, reprinting and re-machining another part. Also, removing the part from the machine would require re-localization and fixturing of the part, which could take significantly longer than probing on the machine.

5.2 Breakeven Analysis for Production Quantity

Fixturing custom components is a constant challenge in any manufacturing environment. Geometrical freedom associated with additive manufacturing creates an even greater challenge when trying to fixture custom components into a CNC machine. Customization of fixtures can take weeks and may cost anywhere between \$50,000 and \$150,000. For this to be economically advantageous, a much larger production quantity than intended by DASH would be necessary. The DASH process eliminates the need for custom fixturing by incorporating sacrificial support material. The unit cost for an additively manufactured part is approximately \$1200 (Laureijs et al., 2017), but we know that the part with support requires more material and time to produce. Assume that this extra material and time increases the cost per unit by 33% or \$400 for the part described. The same part printed with sacrificial supports is now estimated to cost \$1600. To justify the use of a custom fixture instead of a DASH printed component, breakeven analysis suggests that at least 125 units would need to be printed to recover the cost of a fixture which costs \$50,000; 375 units would need to be manufactured to recover the cost of a \$150,000 fixture. Let N be the number of units produced. Equations (4)–(5) show the breakeven calculations.

To obtain a lowerbound on the breakeven quantity, assume a fixture cost of \$50,000, then solving

$$\$1,200N + \$50,000 = \$1,600N \tag{4}$$

gives a lower bound of $N = 125$ units. The upperbound on the breakeven quantity is achieved assuming a fixture cost of \$150,000 such that

$$\$1,200N + \$150,000 = \$1,600N, \tag{5}$$

which implies a breakeven quantity of $N = 375$ units.

Since DASH is designed for extremely low production runs (less than 10), the use of a custom fixture is not economically advantageous. Assuming only 10 parts will be produced, the cost of a custom fixture would need to be less than \$4,000 to be economically advantageous over the DASH process. Equation (6) shows calculation for breakeven fixture cost. Let X be the cost of a custom fixture to breakeven producing 10 parts.

$$\$1,200\,(10 \text{ units}) + X = \$1,600\,(10 \text{ units}) \tag{6}$$

The actual cost of manufacturing one custom AM component using traditional fixation techniques would be equal to the cost of printing the part plus the cost of the fixture plus the cost of actual machine time and inspection. We will assume that the actual machine time and inspection would be equal for the traditional method and the DASH method. To produce one custom component using traditional fixation methods, the cost for one unit could be over \$100,000 due to the high fixed cost in creating a fixture. This is more than 60 times the cost to machine the same part created through the DASH method.

5.3 Engineering Cost Reductions

Inspection planning procedures are commonly created by engineers or other quality control specialists to ensure that parts are created to specifications called out in tolerance drawings. The automatic inspection system described in this work automatically collects feature and tolerance callout data from part model files, generates a probing inspection plan with toolpaths, and compares the results to the callouts. This automatic inspection generation would drastically reduce the amount of time an engineer needs to spend developing inspection plans and toolpaths. This would allow the engineer to perform other value-added tasks during the time they previously would have devoted to inspection planning. Hourly engineer costs (E_c) are estimated as the annual salary paid to an engineer (\$100,000 per year) divided by the number of hours worked per year (2000 hrs per year) (Bureau of Labor Statistics, 2022; CareerOneStop, 2022).

$$E_c = \frac{\$100,000 \text{ per year}}{2000 \text{ hrs per year}} = \$50 \text{ per hour} \tag{7}$$

If inspection planning time could be reduced from 60 minutes per part to 5 minutes per part using the automatic system, this would result in direct savings of \$45.83 per part in engineering costs. This does not account for the potential monetary benefit to a company that could also be realized during the 55 extra minutes of free time the engineer could reallocate.

5.4 Lead Time Reduction

The DASH process also provides a significantly faster way to create a custom fixation method for complicated parts. The DASH process including printing of parts can be completed start to finish in just a few hours. Printing time for metal components may take up to one to two days for large builds. Creation of custom fixtures for machining can take more than four weeks to produce. Reducing from four weeks to two days would be equivalent to a 92% reduction in lead time. This shows that the reduced lead time to create custom components through DASH is also favored over traditional fixation methods.

Reducing lead time has a significant impact on the costs to a company. Lead time reductions result in less inventory, higher customer satisfaction, less down time or non-value-added time, and potentially increased productivity of employees. The economic advantage of the DASH process becomes apparent in the reduction of inventory alone. This process provides a way to completely fulfill a customer order for a specific component in a matter of days without needing to hold excessive inventory to maintain a high service level.

5.5 Setup Time Reduction

There is currently still significant setup time required to localize the part into the machine in the DASH process. Laser scanning the part for localization, as described in Section 3, took approximately 35 minutes. Actual machine time for one cylindrical bore was only about 12 minutes, and the machining parameters were somewhat conservative compared to those which would be used by an actual production environment. For this example part, the setup time was significantly greater than the actual machining time. Another DASH created part with significantly more machining surfaces took approximately 167 minutes to completely machine. This part had a similar localization time of approximately 35 minutes. Even this example shows that setup was approximately 17% of the entire machining process. If the part is removed from the machine for any reason, including off machine inspection, scanning would be necessary to re-localize the part in the CNC machine. For production environments, this is a large amount of downtime for a machine which would be utilized for something else.

There are systems in place which could automate the localization of DASH parts. Scanning probes are commercially available from companies such as Renishaw. These probes can collect hundreds of sample points per second, providing extremely detailed information about surface profiles and location of parts within machines. Similarly, laser scanning could be performed by an automatic robotic system to rapidly decrease the time it takes to scan (Wang and Fang, 2015; Wu et al., 2017). Son et al. (2002) even present a method for automatic laser scanning of organically shaped parts. Systems to automate the scanning process are expensive, which creates a barrier to apply this technology to the DASH process.

Recall the time to probe is linearly related to the number of sample points with each sample point taking approximately three seconds to complete. Even with the maximum number of sample points (60), the total measurement time was less than 3.6 minutes. This probing time, compared to an example DASH part with machining cycle time of approximately 167 minutes, accounts for only 2% of total machine time.

These sample measurements can be transferred to Microsoft Excel as a text file and passed through the VBA code in under one minute to determine accurate estimates for size and position of the hole. This shows that the maximum time required to collect data about one cylindrical feature would be less than five minutes. Since this five-minute measurement cycle could tell is if a part is out of specification and could be reworked, we eliminate the approximately 35 minutes to re-scan and re-localize the part with respect to the machine. This would result in drastic cost savings in the event of a reworked part.

Assume that a part with a cylindrical bore feature is machined through the DASH method. After machining initially, CMM inspection occurs and determines that the cylindrical feature is not within tolerance but could be re-machined to meet specifications. Time between existing process and proposed process can be compared in Table 5 below. Times are approximate values from experience executing the DASH process. Note that machining time is highly dependent on the complexity of the part and the number of critical features to be machined.

This suggests that approximately 67 minutes could be saved by utilizing the on-machine measurement system described in this research. That equates to a 33% reduction in total process time and would therefore result in reduced costs. If production costs were estimated to be $300 per hour to account for machine time, tool wear, overhead, utilities, and operator salary, we could expect approximately $335 in savings per part just by reducing the localization time.

Table 5: Time comparison in minutes between the existing process and the new process proposed in this paper.

Process Step Time (min)	Current	Proposed
Setup (localization)	35	35
Toolpath Generation	10	10
Machining	60	60
Off Machine Inspection (CMM)	30	N/A
Re-Localization	35	N/A
New Toolpath Generation	10	10
Re-Machining	10	10
Off Machine Inspection (CMM)	10	N/A
On Machine Inspection (OMM)	N/A	4
Total Time (min)	**200**	**133**

This OMM strategy results in direct cost savings from reduced machine and operator time. The success of this qualification method also justifies the use of the DASH method as a replacement for traditional manufacturing processes to create custom metal parts with critically toleranced features. Reductions in lead time, machine time, inventory costs, and fixturing costs for low volume production runs all suggest that the DASH process with this inspection method is an economically viable solution to custom production needs.

6 Summary of Guidelines

6.1 Production Quantity

From the economic analysis in Section 5, we know that depending on the fixed cost to produce a custom fixture DASH is the cheaper production method in low quantities. Given the lower and upper bounds on the cost to produce a fixture of $50,000 and $150,000 DASH is economically advantageous when less than 125 or 375 units are produced, respectively. With this information it is recommended that the DASH process be utilized for production runs less than 125 units. Similar computations to those performed in Equations (4)–(5) can be recalculated given the estimated fixed cost for a particular part fixture.

6.2 Measurement Sampling Strategy

As described in Section 3, Methods M2, M3, M5, and M6 are statistically similar in their ability to measure features. Any of these four methods are shown to be viable options when sampling. However, there is a possibility to have clustered sampling locations using the completely randomized method M6. For this reason, special attention should be placed on the generated toolpath angles and Z heights when using method M6.

The bird-cage sampling strategy could also provide skewed results for defects which occur in a recurring pattern. It is possible for the sampling points to occur at the same locations as the repetitive defects. For this reason, it is recommended to visually inspect features for repetitive defects and ensure none exist before utilizing the bird-cage method M2. However, results from the case study show that this method can accurately calculate the size and position of cylindrical features while also minimizing the variance between measurements. Estimated parameter values converge after approximately 30 sample points, but given the short time to sample additional points, 40 points per feature are recommended to ensure accuracy. An additional 30 seconds of sampling time is insignificant when compared to the few weeks of lead time which may be considered when creating a traditional fixation device. The 40 sample points should be fairly evenly distributed between both number of points measured per Z height and the number of Z heights taken. A sufficient strategy could be eight sample points per Z height at each of five Z heights.

6.3 Acceptance conditions for feature accuracy

From the case study provided, we know that it is possible to create confidence intervals smaller than 0.025mm (0.001") in magnitude around estimates for R, C, and C'. For this reason, all values in the confidence interval should fall within the allowable range of values that the cylindricity or position tolerance callouts specify. If any value in the estimated confidence interval falls outside this range, we should fail to accept that the feature is within tolerance.

7 Conclusion

This research implements a method to automatically inspect cylindrical bores on AM parts with critically tolerance surfaces. Testing shows that on machine measurement is a valid strategy for part inspection using a touch probe. Both acceptable and unacceptable parts can be detected using this strategy. Toolpaths can be automatically generated using the information stored in the AMF-TOL file in conjunction with the transformation information created during the DASH process. The DASH process is economically advantageous to traditional AM processes with custom fixation for low volume production runs. OMM further improves the financial advantage by reducing setup time needed for inspection.

Acknowledgements

The last author was supported by a grant from the US Army Research Office (grant # W911NF1910055).

References

3DEO (2022). Cost savings on the rise as a key benefit of 3D printing. 3DEO website, Accessed 21 October 2023, https://www.3deo.co/metal-3d-printing/cost-savings-on-the-rise-as-a-key-benefit-of-3d-printing/.

Bromberger, J., Ilg, J., and Miranda, A. (2022). The mainstreaming of additive manufacturing. McKinsey & Company website, Accessed 20 October 2023, https://www.mckinsey.com/capabilities/operations/our-insights/the-mainstreaming-of-additive-manufacturing.

Bureau of Labor Statistics (2022). US Department of Labor, Occupational Outlook Handbook, Industrial Engineers. https://www.bls.gov/ooh/architecture-and-engineering/industrial-engineers.htm.

CareerOneStop (2022). Salary finder tool. https://www.careeronestop.org/Toolkit/Wages/.

Chen, N., Barnawal, P., and Frank, M. (2018). Automated post machining process planning for a new hybrid manufacturing method of additive manufacturing and rapid machining. *Rapid Prototyping Journal*, 24(7):1077–1090.

Deere (2022). John Deere website. https://www.deere.com.

FARO (2019). FARO Edge ScanArm website. Accessed 15 May 2019, https://www.faro.com/resource/faro-edge-scanarm-hd/.

FARO (2023). What is GDT? Accessed 25 January 2023, https://www.faro.com/en/Resource-Library/Article/what-is-gdt.

Frank, M., Wysk, R., and Joshi, S. (2005). Rapid Planning for CNC Milling - A new approach for rapid prototyping. *Journal of Manufacturing Systems*, 23(3):242–255.

Frank, M., Wysk, R., and Joshi, S. (2006). Determining Setup Orientations From the Visibility of Slice Geometry for Rapid Computer Numerically Controlled Machining. *Journal of Manufacturing Science and Engineering*, 128(1):228–238.

Haas (2019). Haas VF-3 website. Accessed 22 Apr 2019, https://www.haascnc.com/machines/vertical-mills/vf-series/models/medium/vf-3.html.

International Organization for Standardization (ISO) (2023). ISO website. Accessed 10 February 2023, https://www.iso.org/home.html.

Janecki, D., Zwierzchowski, J., and Cedro, L. (2015). A problem of optimal cylindricity profile matching. *Bulletin of the Polish Academy of Sciences*, 63(3):771–779.

Keefer, N. (2020). The cost impact of additive manufacturing. Perception Engineering blog dated 6 July 2020, Accessed 21 October 2023, https://www.perceptioneng.com/blogold/the-cost-impact-of-additive-manufacturing.

Kelly, C. (2018). Automatic feature based inspection and qualification for additively manufactured parts with critical tolerances. Masters thesis, Industrial & Systems Engineering, North Carolina State University, http://www.lib.ncsu.edu/resolver/1840.20/35690.

Khajavi, S., Holmstr om, J., and Partanen, J. (2018). Additive manufacturing in the spare parts supply chain: hub configuration and technology maturity. *Rapid Prototyping Journal*, 24(7):1178–1192.

Kramer, C. (1956). Extension of multiple range tests to group means with unequal numbers of replications. *Biometrics*, 12(3):307–310. https://doi.org/10.2307/3001469.

Laureijs, R., Roca, J., Narra, S., Montgomery, C., Beuth, J., and Fuchs, E. (2017). Metal additive manufacturing: Cost competitive beyond low volumes. *Journal of Manufacturing Science and Engineering*, 139(8):1–9.

LEADRP (2022). GDT: A Detailed Introduction to Geometric Dimensioning and Tolerancing. Accessed 25 January 2023, https://leadrp.net/blog/gdt-a-detailed-introduction-to-geometric-dimensioning-and-tolerancing/.

Li, Y., Cheng, Y., Hu, Q., Zhou, S., Ma, L., and Lim, M. (2019). The influence of additive manufacturing on the configuration of make-to-order spare parts supply chain under heterogeneous demand. *International Journal of Production Research*, 57(11):1–20. https://doi.org/10.1080/00207543.2018.1543975.

Lăzureanu, C. (2014). Spirals on surfaces of revolution. *VisMath*, 16(2):1–10. http://elib.mi.sanu.ac.rs/files/journals/vm/57/vmn57p2-10.pdf.

Manogharan, G. (2014). Hybrid Manufacturing: Analysis of Integrating Additive and Subtractive Methods. PhD Dissertation, Industrial & Systems Engineering, North Carolina State University, Raleigh, NC, USA. http://www.lib.ncsu.edu/resolver/1840.16/9663.

Manogharan, G., Wysk, R., Harrysson, O., and Aman, R. (2015). AIMS- a Metal Additive-Hybrid Manufacturing System: System Architecture and Attributes. In Shih, A. and Wang, L., editors, *43rd North American Manufacturing Research Conference, NAMRC 43*, volume 1 of *Procedia Manufacturing*, pages 273–286. Charlotte, NC, JUN 08-12, 2015.

Manogharan, G., Wysk, R. A., and Harrysson, O. L. (2016). Additive manufacturing–integrated hybrid manufacturing and subtractive processes: economic model and analysis. *International Journal of Computer Integrated Manufacturing*, 29(5):473–488.

Mastercam (2021). Mastercam website. Accessed 10 Nov 2021, https://www.mastercam.com/.

Mazak (2019). Mazak integrex i-100 website. Accessed 22 Apr 2019, https://www.mazakusa.com/machines/integrex-i-100/.

Renishaw (2008). Inspection Plus software for Haas machining centres. Programming manual H-2000-6222-0A-B, Accessed 22 Apr 2019, https://staging-diy.haascnc.com/sites/default/files/Locked/2/Renishaw_Programming_Manual_H_2000_6222_0A_B.pdf.

Renishaw (2023). Renishaw RMP600 Probe Kit website. Accessed 10 February 2023, https://renishawprobe.com/p/machine-tool/A-5312-0001.

SAS (2019). JMP website. Accessed 22 Apr 2019, https://www.jmp.com/en_us/home.html.

Son, S., Park, H., and Lee, K. (2002). Automated laser scanning system for reverse engineering and inspection. *International Journal Of Machine Tools And Manufacture*, 42(8):889–897.

Srinivasan, H. (2014). Automated model processing and localization of additively manufactured parts for finish machining. PhD Dissertation, Industrial & Systems Engineering, North Carolina State University, Raleigh, NC, USA. http://www.lib.ncsu.edu/resolver/1840.16/11254.

Srinivasan, H., Harrysson, O., and Wysk, R. (2015a). Automatic part localization in a CNC machine coordinate system by means of 3D scans. *International Journal of Advanced Manufacturing Technology*, 81:1127–1138. https://doi.org/10.1007/s00170-015-7178-z.

Srinivasan, H., Harrysson, O., and Wysk, R. (2015b). Features and tolerances in additive manufacturing - an extension to the AMF file format. APSE Spring Topical meeting on Achieving Precision Tolerances in Additive Manufacturing. American Society for Precision Engineering, Presentation and Extended Abstract, April 26–29, Raleigh, NC, USA.

Tatham, S. (2021). PuTTY website. Accessed 10 Nov 2021, https://www.putty.org/.

Traband, M., Medeiros, D., and Chandra, M. (2004). A statistical approach to tolerance evaluation for circles and cylinders. *IIE Transactions*, 36(8):777–785.

Tukey, J. (1949). Comparing individual means in the analysis of variance. *Biometrics*, 5(2):99–114. https://doi.org/10.2307/3001913.

Wang, Y. and Fang, H. (2015). A rotating scan scheme for automatic outlier removal in laser scanning of reflective surfaces. *The International Journal Of Advanced Manufacturing Technology*, 81(1):705–716.

Wu, X., Li, Z., and Wen, P. (2017). An automatic shoe-groove feature extraction method based on robot and structural laser scanning. *International Journal of Advanced Robotic Systems*, 14(1):1–14.

Yang, Z., Wysk, R., and Joshi, S. (2012). Setup planning for six-axis wire electric discharge machining. *Journal of Manufacturing Science and Engineering*, 134(2). https://doi.org/10.1115/1.4005801.

Yang, Z., Wysk, R. A., and Joshi, S. (2011). Global Tangent Visibility Analysis for Polyhedral Computer Aided Design Models. *Journal of Manufacturing Science and Engineering*, 133(3). https://doi.org/10.1115/1.4004141.

Yang, Z., Wysk, R. A., Joshi, S., Frank, M., and Petrzelka, J. (2009). Conventional Machining Methods for Rapid Prototyping and Direct Manufacturing. *International Journal of Rapid Manufacturing*, 1(1):41–64.

ORCID iD

Russell E. King https://orcid.org/0000-0003-4576-6600

Brandon M. McConnell https://orcid.org/0000-0003-0091-215X

Appendix

Sampling Strategies

In addition to the Method M2 (birdcage) approach from Figure 4 and Method M7 (spiral) in Figure 5, we tested the remaining strategies in Table 2 , illustrated in Figures 11–15.

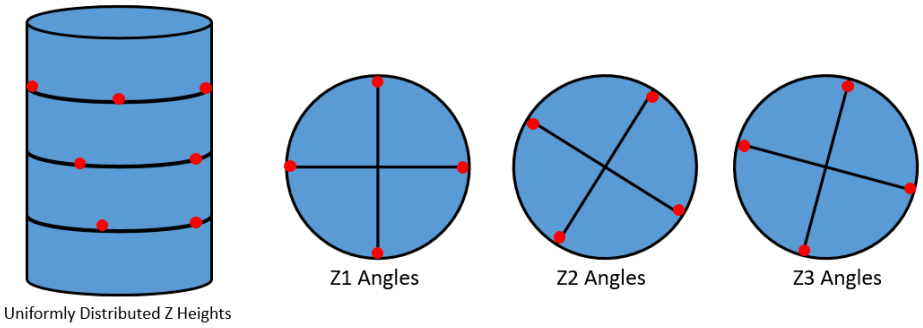

Figure 11: Method M1 sampling strategy.

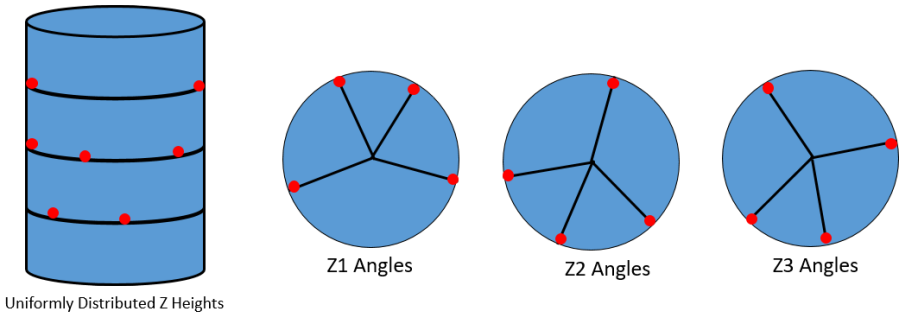

Figure 12: Method M3 sampling strategy.

Toolpath Technical Details

Formatting details for the probing cycle are provided in the Renishaw Programming Manual (Renishaw, 2008): **G65 P9821 Aa Dd**, using a as the angle for vector measurement counterclockwise from the $X+$ axis direction as 0 and d as the nominal radial distance to surface. When the Renishaw probing cycle is executed, radius measurement values are stored as variable #188 in the Haas VF3 (Haas, 2019).

When the Renishaw O9821 single point angled surface measurement macro is run, variable #188 is populated with the measured bore radius. Then we can set an empty macro variable, #600, equal to #188. If successive measurements are performed, unique macro variables are used to save each sample measurement. Finally, we can DPRNT these variables to record them as our sample radii measurements. Since the CNC code must contain an input for the angle in which to measure, these direction vectors are known and will be used later to calculate true position for cylindrical features. The interested reader should consult Kelly (2018) for additional details.

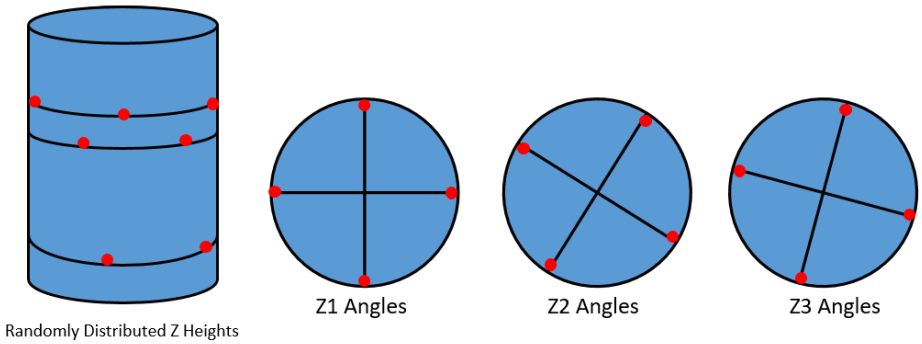

Figure 13: Method M4 sampling strategy.

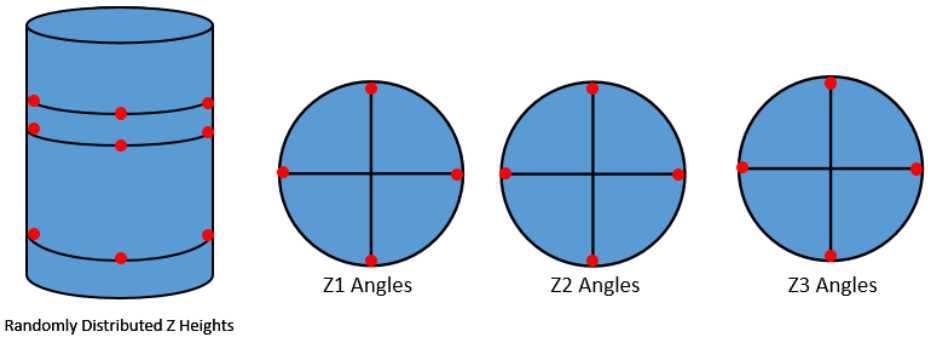

Figure 14: Method M5 sampling strategy.

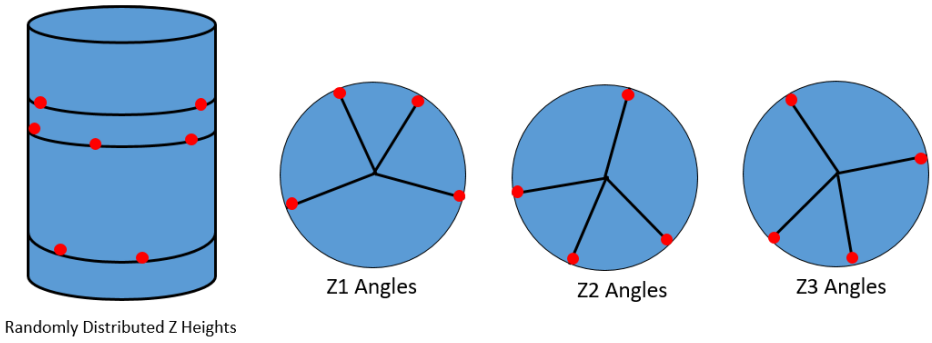

Figure 15: Method M6 sampling strategy (completely randomized).